Will black hole-neutron star binary inspirals tell us about the neutron star equation of state?

Francesco Pannarale,[1] Luciano Rezzolla,[1,2] Frank Ohme,[1] and Jocelyn S. Read[3]

[1]*Max-Planck-Institut für Gravitationsphysik, Albert Einstein Institut, Potsdam, Germany*

[2]*Department of Physics and Astronomy, Louisiana State University, Baton Rouge, Louisiana, USA*

[3]*Department of Physics and Astronomy, The University of Mississippi, University, Mississippi 38677, USA*

(Received 17 March 2011; published 7 November 2011)

The strong tidal forces that arise during the last stages of the life of a black hole-neutron star binary may severely distort, and possibly disrupt, the star. Both phenomena will imprint signatures about the stellar structure in the emitted gravitational radiation. The information from the disruption, however, is confined to very high frequencies, where detectors are not very sensitive. We thus assess whether the lack of tidal distortion corrections in data-analysis pipelines will affect the detection of the *inspiral* part of the signal and whether these may yield information on the equation of state of matter at nuclear densities. Using recent post-Newtonian expressions and realistic equations of state to model these scenarios, we find that point-particle templates are sufficient for the detection of black hole-neutron star inspiralling binaries, with a loss of signals below 1% for both second- and third-generation detectors. Such detections may be able to constrain particularly stiff equations of state, but will be unable to reveal the presence of a neutron star with a soft equation of state.

DOI: 10.1103/PhysRevD.84.104017 PACS numbers: 04.30.Db, 04.25.Nx, 95.30.Sf, 97.60.Jd

I. INTRODUCTION

Coalescing binaries of stellar-mass compact objects, i.e., black holes (BHs) and neutron stars (NSs), are a primary target for gravitational wave (GW) searches performed with kilometer-size laser-interferometric detectors, such as LIGO and Virgo, and one of the most promising for a first detection. Binaries containing at least one NS are particularly interesting because their GW signal contains signatures of the physical conditions of matter at nuclear densities (see, e.g., [1–9]) and may thus eventually reveal the equation of state (EOS) of NSs, which is currently highly uncertain [10].

In the case of BH-NS binaries, in particular, the most relevant of such signatures was traditionally thought to be the GW frequency above which no hydrostatic equilibrium is possible, $f_{\rm tide}$. Because this frequency was identified with the complete tidal disruption of the NS, the GW amplitude was consequently assumed to decay rapidly for larger frequencies [11] and information on the EOS was thought to be inferrable from $f_{\rm tide}$ for binaries in which the NS were to be disrupted before the system reaches the innermost stable circular orbit. This picture was considerably modified by the recent numerical-relativity simulations presented in [12] which, instead, highlighted that $f_{\rm tide}$ effectively marks only the onset of *mass shedding*. The complete tidal disruption, on the other hand, is achieved only later and at higher frequencies, so that the GW spectrum decays exponentially at a cutoff frequency $f_{\rm cutoff} \simeq (1.2 - 1.5) f_{\rm tide}$. Stated differently, in contrast to the expectations of [11], the GW spectrum shows no distinctive feature at the mass-shedding frequency $f_{\rm tide}$; conversely, information on the NS EOS is in principle accessible through $f_{\rm cutoff}$. The two frequencies do not coincide because the tidal disruption is not instantaneous and the GW frequency changes rapidly in time, so that the transition from a chirping signal to an exponentially decaying one is pushed to higher frequencies. The difference between $f_{\rm tide}$ and $f_{\rm cutoff}$ increases as $f_{\rm tide}$ approaches the GW frequency at the innermost stable circular orbit, $f_{\rm ISCO}$ [12].

If recent numerical-relativity simulations have pointed out the importance of the cutoff frequency as a very significant marker of the NS properties, they have also highlighted that the accurate determination of such frequency may only be made through numerical simulations, the computational costs of which are still prohibitive for a complete scan of the space of parameters. Moreover, it will be the inspiral portion of the GW signal that will be fully contained in the most sensitive part of the sensitivity curve of ground-based detectors.

In light of all this, two questions follow naturally. (1) Will the use of point-particle template banks for *inspiral* searches cause a loss in the number of detected signals because of the small but secular tidal effects that develop? (2) Will such effects be large enough to provide us with information about the NS EOS? We address here both questions by computing the GW phase evolution of BH-NS binaries when tidal effects are taken into account and by contrasting it with the one expected when both the BH and NS are treated as point particles. We find that the tidal corrections to the phase evolution depend sensitively on the NS EOS, but also that they are generally small. Hence, present data-analysis pipelines, which do not include tidal corrections, are sufficient for a successful detection of BH-NS inspirals, but only a particularly stiff EOS would mark the GW signal sufficiently for us to determine it.

II. METHODOLOGY

Early inspiral tidal effects may be effectively described in terms of a single EOS-dependent tidal deformability parameter λ [5–7,13] (also indicated as μ_2 [5–7]), defined as the ratio of the quadrupole deformation induced on a star and the static external quadrupolar tidal field inducing the deformation, in this case the tidal field of its companion. The tidal deformability parameter is calculated via a linear axisymmetric $\ell = 2$ static perturbation around the center-of-mass of the star, along the axis connecting the two companions; it depends on the EOS via the NS radius, R, and the $\ell = 2$ apsidal constant, or Love number, k_2, through the relation $\lambda = 2k_2R^5/(3G)$ [14–16]. The $\ell = 2$ tidal deformation is expected to be the dominant source of EOS-dependent modifications to the inspiral phase evolution up to the last few orbits of the inspiral prior to the merger, when the mass shedding takes over; higher order in ℓ and λ, nonlinear, and viscous dissipation corrections are all considerably smaller [6]. The imprint of λ on the inspiral of binary NSs was investigated in [6], which concluded that, at a distance of 100 Mpc and using the inspiral below 450 Hz, AdLIGO would be only be able to constrain λ for an extremely stiff EOS.

In order to estimate the GW phase accumulated during the inspiral of BH-NS binaries due to tidal effects, we follow [13,16], with the obvious difference that only one NS provides the tidal contribution. We also include the first post-Newtonian (1PN) order tidal corrections calculated in [17]. Finally, while in [6] the phase evolution was truncated at 450 Hz (roughly 80% of $f_{\rm ISCO}$ for two NSs with $M_{\rm NS} = 1.4M_\odot$ and $R = 15$ km), we here set the value of the truncation frequency $f_{\rm end}$ to be the smaller of $f_{\rm tide}$ and $f_{\rm ISCO}$. The latter is the frequency yielded by the minimum of the post-Newtonian (PN) energy function (see below), while $f_{\rm tide}$ is determined using the relativistic toy model recently discussed in [18], which reproduces numerical-relativity results for $f_{\rm tide}$ within $\lesssim 1\%$. In such a model the NS is described as an ellipsoid which deforms during the inspiral under the effect of the BH tidal field and its internal forces; this is consistent with the approach of [6], since only the $\ell = 2$ tidal deformations are considered.

We contrast the point-particle description of the quadrupole GW phase ($\phi_{\rm PP}$) with the one obtained for a deformable, finite-size NS (ϕ_λ) by integrating the tidal corrections to $d\phi/dx$, where x is the PN expansion parameter, up to 1PN (relative) order [17], i.e., we compute $\Delta\phi \equiv \phi_{\rm PP} - \phi_\lambda$ (which is positive, due to the attractive nature of the tidal coupling). We moreover determine the quadrupole mode of the gravitational radiation in the frequency domain $\tilde{h}(f)$. We use the inspiral part of spinning binary hybrid wave forms [Sec. III of [19]], augmenting the TaylorF2 phase ψ with λ-dependent tidal corrections up to 1PN (relative) order [Eqs. (3.8) in [17]]. The PN expressions in [19] are derived from a 3PN expansion of the binding energy of the system and a 3.5PN (relative order) expansion of the GW energy flux [Eqs. (3.3)-(3.4) in [19]], within the commonly used stationary phase approximation [20]; spin terms are included up to 2.5PN order in phase and 2PN order in amplitude. We use the TaylorT4 [21] description to replace the dx/dt in

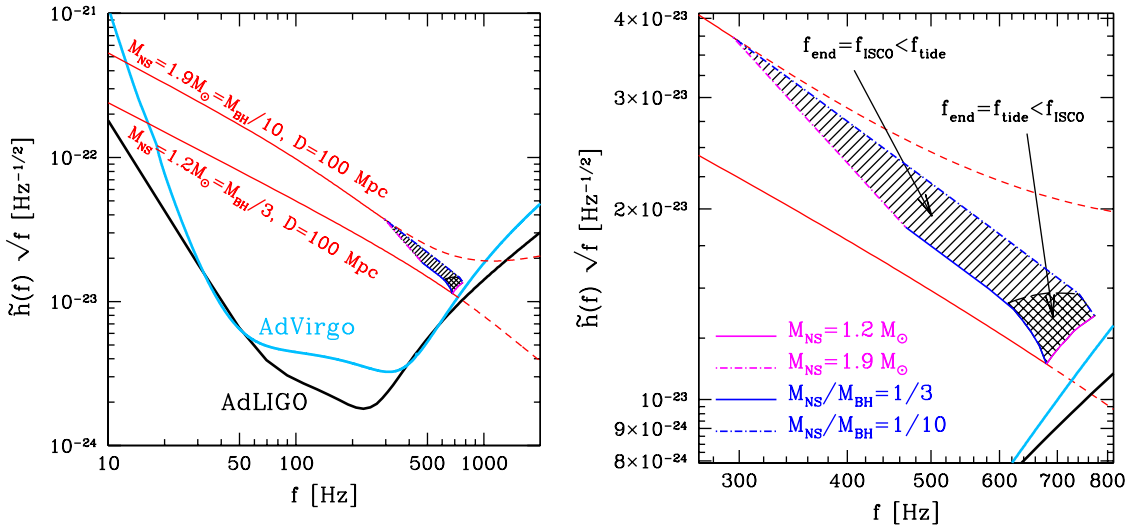

FIG. 1 (color online). Tracks of inspiralling BH-NS binaries at 100 Mpc, for $a = 0$ and a PS EOS (red lines), and their position with respect to the sensitivities of AdLIGO (black line) and AdVirgo (light blue line). To avoid cluttering, we show only the strongest and the weakest signals, which refer to a $1.9M_\odot$ and a $1.2M_\odot$ NS, respectively, in binaries with mass ratio $q = 0.1$ and $q = 1/3$. Each track is terminated at $(f_{\rm end}, \tilde{h}(f_{\rm end})\sqrt{f_{\rm end}})$; the red dashed continuations are shown only for reference. The shaded region is the one spanned by all the termination points obtained by varying $M_{\rm NS}$ and q. A magnification reporting the lines at constant $M_{\rm NS}$ and q that limit the shaded area is shown in the right panel.

the expression of the amplitude A. Even though leading-order tidal contributions are of 5PN order, as opposed to the point-particle terms which are kept up to 3PN or 3.5PN order, their coefficients "compensate" the smallness due to their PN order, making them comparable to 3PN and 3.5PN terms (see [14,17] for detailed discussions). We perform all integrations in the frequency domain, from $f_{\rm start} = 10$ Hz (roughly the low-frequency cutoff of AdLIGO/AdVirgo) to $f_{\rm end} = \min(f_{\rm tide}, f_{\rm ISCO})$.

The free parameters of our model are the NS (barotropic) EOS, the NS mass $M_{\rm NS}$, which ranges between $1.2M_\odot$ and the EOS-dependent maximum value $M_{\rm max}$, the binary mass ratio $q \equiv M_{\rm NS}/M_{\rm BH}$, which we vary between $1/10$ and $1/3$ [22], and the dimensionless BH spin parameter a, which is taken to be (anti-)aligned with the orbital angular momentum (equatorial inspirals). To bracket the possible impact of the EOS on BH-NS inspirals and their GW radiation, we consider three EOSs dubbed APR, GNH3, and PS, respectively. Our choice is motivated by the fact that the APR EOS [23] is based on nuclear many-body calculations, may be favored by the observations [24], and yields NSs with low λ; the GNH3 EOS [25], on the other hand, is based on mean-field theory and yields intermediate λ; finally, the "liquid" version of the PS EOS [26] is somewhat dated but yields rather high λ. The set chosen, therefore, covers the relevant range of stiffness (APR being the softest and PS the stiffest) and can be considered representative of a much larger sample of EOSs. Note that all of these EOSs have a maximum mass $1.93 \lesssim M_{\rm max}/M_\odot \lesssim 2.66$.

Figure 1 illustrates the role played by $f_{\rm end}$. We consider the PS EOS and nonspinning BHs and show the tracks of inspiralling BH-NS binaries at 100 Mpc (red solid lines), along with the sensitivity curves of AdLIGO (black line) and AdVirgo (light blue line). The signal amplitudes are averaged over sky location and relative inclination of the binary. We show explicitly only the strongest and weakest signal, which refer to $M_{\rm NS} = 1.9M_\odot$, $q = 0.1$ and to $M_{\rm NS} = 1.2M_\odot$, $q = 1/3$, respectively. The tracks terminate at $(f_{\rm end}, \tilde{h}(f_{\rm end})\sqrt{f_{\rm end}})$ and their continuations as red dashed lines serve only as a reference. The shaded region, which is magnified in the right panel, is the one spanned by the termination point for all combinations of $M_{\rm NS}/M_\odot \in [1.2, 1.9]$ and $q \in [0.1, 1/3]$.

III. DEPHASING AND OVERLAPS

Once a binary with parameters $(q, a, M_{\rm NS}, \lambda)$ is selected, we compute $\Delta\phi(f_{\rm end})$. Overall, we find that $\Delta\phi$: (i) is greater for bigger λ's, i.e., for more deformable NSs (see Fig. 2); (ii) grows with q, i.e., for comparable masses; (iii) decreases as $M_{\rm NS}$ [cf. Eq. (21) in [6]]; (iv) depends only weakly on the BH spin, since the only spin dependence may come through $f_{\rm end}$, but binaries with $f_{\rm end} = f_{\rm tide} < f_{\rm ISCO}$ are hardly affected, since $f_{\rm tide}$ is not very sensitive to a, while binaries with $f_{\rm end} = f_{\rm ISCO} < f_{\rm tide}$ are those with high $M_{\rm NS}$ and low λ, so that the gain or loss in $f_{\rm ISCO}$ does not modify $\Delta\phi$ significantly.

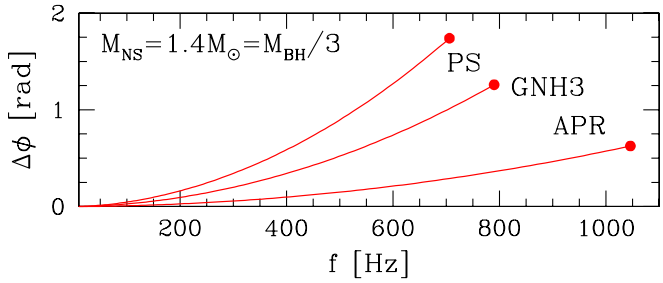

FIG. 2 (color online). Tidal distortion contribution to the quadrupole GW phase $\Delta\phi$ for the three representative EOSs. The tracks end at $f_{\rm end}$ and yield larger dephasings for stiffer EOSs, such as PS.

To determine whether the dephasings found may affect the detection of BH-NS inspiral events, we compute, for each binary, the *overlap* between the point-particle model of the GW inspiral signal ($h_{\rm PP}$) and the one which includes tidal deformability effects (h_λ); this is the normalized inner product of the two signals, maximized over time and phase shifts, i.e., $\mathcal{O}[h_{\rm PP}, h_\lambda] \equiv \max_{\{t_0,\phi_0\}} \frac{\langle h_{\rm PP}|h_\lambda\rangle}{\sqrt{\langle h_{\rm PP}|h_{\rm PP}\rangle\langle h_\lambda|h_\lambda\rangle}}$, where the inner product is $\langle h_{\rm PP}|h_\lambda\rangle \equiv 4\Re\int_{f_{\rm start}}^{f_{\rm end}} df \frac{\tilde{h}_{\rm PP}(f)\tilde{h}_\lambda^*(f)}{S_n(f)}$, $S_n(f)$ being the noise power spectral density of a chosen detector. Note that we are implicitly assuming that the wave forms including tidal effects are the "real" signals and treating the point-particle wave forms as the templates used to detect them.

Our results for the three EOSs considered and a BH with $a = 0$ are shown in Fig. 3 for AdLIGO. Note that for any EOS choice and for any combination of the BH and NS

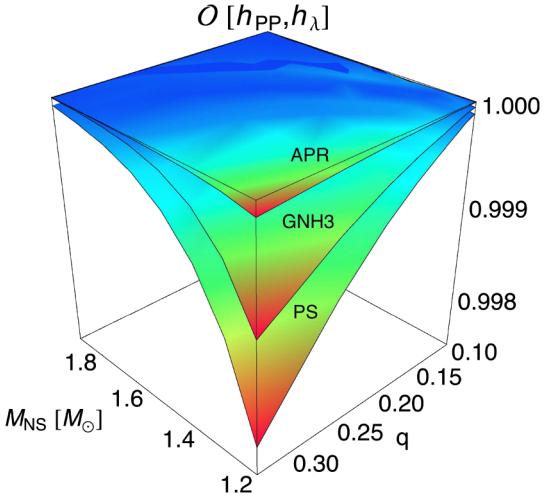

FIG. 3 (color online). Overlaps between PN wave forms for BH-NS binary systems modeled as point particles and with the inclusion of tidal distortion effects ("λ"). The overlap is calculated for the AdLIGO detector and for nonspinning BHs.

masses, the overlap is always greater than 0.997, which corresponds to a 1% loss of signals; this is true even for spins up to $a = 1$. The smallest overlap is given by the PS EOS combined with $M_{\rm NS} = 1.2M_\odot$, $q = 1/3$ (the leading-order tidal contribution to the phase $\psi(f)$ being $\propto \frac{(12+q)q^{4/3}}{(1+q)^{4/3}} f^{5/3}$), and $a = 1$ (inclusion of spin changes overlaps by $<10^{-3}$). Hence, even if all binaries were to have these extreme properties, the loss of signals would be less than 1%. All in all, BH-BH inspiral templates will allow second-generation interferometers to detect inspiralling BH-NS binaries with less than a 1% loss of signals. Similar results hold for the third-generation detector Einstein Telescope (ET) [27], with a minimum possible overlap of about 0.995.

IV. MEASURABILITY

Determining that the fraction of lost signals is below 1% does not address the question of whether the detected signals may be used to learn about the EOS. To address this point, we consider a nominal detector-binary distance of 100 Mpc and calculate the distinguishability as $\delta h_{{\rm PP},\lambda} \equiv \langle h_{\rm PP} - h_\lambda | h_{\rm PP} - h_\lambda \rangle \gtrsim 2(1 - \mathcal{O}[h_{\rm PP}, h_\lambda])\rho^2$, where $\rho^2 = \langle h_{\rm PP} | h_{\rm PP} \rangle \simeq \langle h_\lambda | h_\lambda \rangle$ is the signal-to-noise-ratio (SNR) and we neglected the term $\langle h_{\rm PP} | h_{\rm PP} \rangle - \langle h_\lambda | h_\lambda \rangle \sim 10^{-4}$. Since we treat $h_{\rm PP}$ as the "template" and h_λ as the "signal," a necessary (but not sufficient) condition to distinguish between the two is that $\delta h_{{\rm PP},\lambda} > 1$ [28]. Clearly, the greater $\delta h_{{\rm PP},\lambda}$, the higher the chances of measuring the tidal effects.

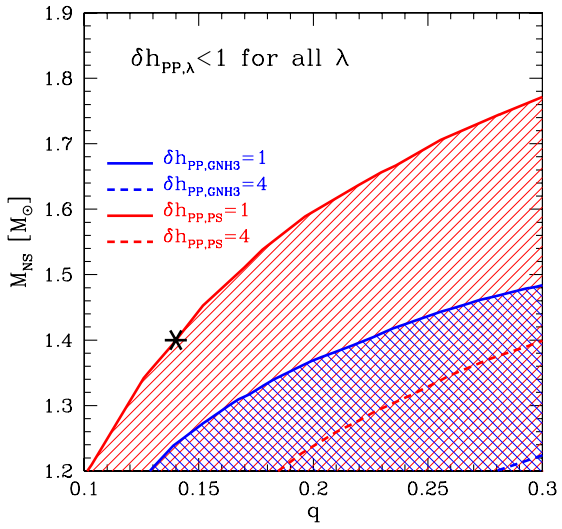

FIG. 4 (color online). Distinguishability $\delta h_{{\rm PP},\lambda}$ by AdLIGO for binaries at 100 Mpc and with $a = 0$. In the white area $\delta h_{{\rm PP},\lambda} < 1$ for all EOSs, in the red-shaded one $\delta h_{\rm PP,PS} > 1$, and in the blue-shaded one $\delta h_{\rm PP,GNH3} > 1$. Contours for $h_{{\rm PP},\lambda} = 1, 4$ are shown for both EOSs. The black star marks a canonical $10M_\odot - 1.4M_\odot$ BH-NS binary.

In Fig. 4, we consider AdLIGO and report $\delta h_{{\rm PP},\lambda}$ for binaries with $a = 0$. In calculating the distinguishability, we average the signal amplitudes both over sky location and over relative inclination of the binary. Note the existence of a region where $\delta h_{{\rm PP},\lambda} < 1$ for all EOSs (white area) in the space of parameters (q, $M_{\rm NS}$); this indicates that the inspiral of BH-NS binaries falling in this region will not be distinguishable from a BH-BH inspiral. For larger mass ratios and smaller NS masses, $\delta h_{{\rm PP},\lambda}$ increases, becoming equal to 1 first for the PS EOS (red-shaded area) and then for the less stiff GNH3 EOS (blue-shaded area). The maximum value of $\delta h_{{\rm PP},\lambda}$ is ~ 10 (~ 5) for the PS (GNH3) EOS. Note that the black star pin-points a canonical $10M_\odot - 1.4M_\odot$ BH-NS binary and that, for the popular APR EOS, $\delta h_{\rm PP,APR} < 1$ for any (q, $M_{\rm NS}$); we briefly mention that even if we push our calculations to $q < 1$ (bearing in mind that the model of [18] should break down for such high q's), $\delta h_{\rm PP,APR}$ hardly reaches 2 for this EOS. However, an APR(-like) EOS may become measurable if the binary is optimally oriented and/or is less than 100 Mpc away. The PS, GNH3, and APR EOS are (marginally) distinguishable by AdLIGO within a range of 310, 225, and 75 Mpc, respectively, for a $3.6M_\odot$-$1.2M_\odot$ BH-NS binary.

To test the robustness of our results, we repeated all calculations after artificially decreasing $f_{\rm end}$ by 20%. Even though the overlaps (distinguishabilities) increased (decreased) a little (e.g, the minimum overlap increased by less than 10^{-3} and the regions in which $h_{{\rm PP},\lambda} \gtrsim 1$ were practically unmodified), our conclusions remained unchanged, thus suggesting that our results are robust even for non-negligible changes of $f_{\rm end}$.

V. CONCLUSIONS

The use of point-particle templates to detect BH-NS inspirals leads to a loss of detected signals which is below 1% for both AdLIGO/AdVirgo and ET. Moreover, for binaries at 100 Mpc, AdLIGO/AdVirgo will essentially be "blind" to tidal effects if superdense matter follows an APR-like EOS and may be able to reveal them only for NSs with a particularly stiff EOS and in large-mass-ratio binaries. This scenario improves for a more sensitive detector such as ET. In this case, the larger SNRs lead to a 2-order-of-magnitude gain in $\delta h_{{\rm PP},\lambda}$, so that even soft EOSs, like APR, are distinguishable.

A final remark should be made. The results presented here make use of the most accurate PN expressions available to date and the comparisons made with and without tidal corrections remove in part the problem of systematic biases in the PN formulation, which could be large for $q \lesssim 1$. Yet, they do not account for higher-order deformation corrections which could amplify tidal parameters [7,9], and nonlinear responses to the tidal field, such

as those produced by crust fracturing or resonant tidal excitation of stellar modes [29]. Although these contributions should yield only fractional corrections to the already small dephasings, either increasing or decreasing them, it is only their proper inclusion that will provide conclusive limits on the tidal effects that affect the inspiral signal.

ACKNOWLEDGMENTS

It is a pleasure to thank E. Berti, T. Damour, T. Hinderer, A. Nagar, B. S. Sathyaprakash, and A. Tonita for carefully reading the manuscript. This work was supported in part by the DFG grant SFB/Transregio 7, by ''CompStar,'' a Research Networking Programme of the European Science Foundation, and by NSF Grant No. PHY-0900735.

[1] L. Baiotti, B. Giacomazzo, and L. Rezzolla, Phys. Rev. D **78**, 084033 (2008).
[2] M. D. Duez, F. Foucart, L. E. Kidder, C. D. Ott, and S. A. Teukolsky, Classical Quantum Gravity **27**, 114106 (2010).
[3] K. Kyutoku, M. Shibata, and K. Taniguchi, Phys. Rev. D **82**, 044049 (2010).
[4] B. Giacomazzo, L. Rezzolla, and L. Baiotti, Mon. Not. R. Astron. Soc. **399**, L164 (2009).
[5] T. Damour and A. Nagar, Phys. Rev. D **80**, 084035 (2009).
[6] T. Hinderer, B. D. Lackey, R. N. Lang, and J. S. Read, Phys. Rev. D **81**, 123016 (2010).
[7] T. Damour and A. Nagar, Phys. Rev. D **81**, 084016 (2010).
[8] L. Rezzolla, L. Baiotti, B. Giacomazzo, D. Link, and J. A. Font, Classical Quantum Gravity **27**, 114105 (2010).
[9] L. Baiotti, T. Damour, B. Giacomazzo, A. Nagar, and L. Rezzolla, Phys. Rev. Lett. **105**, 261101 (2010).
[10] J. M. Lattimer and M. Prakash, Phys. Rep. **442**, 109 (2007).
[11] M. Vallisneri, Phys. Rev. Lett. **84**, 3519 (2000).
[12] M. Shibata and K. Taniguchi, Phys. Rev. D **77**, 084015 (2008).
[13] É. É. Flanagan and T. Hinderer, Phys. Rev. D **77**, 021502 (2008).
[14] T. Mora and C. M. Will, Phys. Rev. D **69**, 104021 (2004).
[15] E. Berti, S. Iyer, and C. M. Will, Phys. Rev. D **77**, 024019 (2008).
[16] T. Hinderer, Astrophys. J. **677**, 1216 (2008).
[17] J. Vines, E. E. Flanagan, and T. Hinderer, Phys. Rev. D **83**, 084051 (2011).
[18] F. Pannarale, A. Tonita, and L. Rezzolla, Astrophys. J. **727**, 95 (2011).
[19] L. Santamaría *et al.*, Phys. Rev. D **82**, 064016 (2010).
[20] B. S. Sathyaprakash and S. V. Dhurandhar, Phys. Rev. D **44**, 3819 (1991).
[21] T. Damour, B. R. Iyer, and B. S. Sathyaprakash, Phys. Rev. D **63**, 044023 (2001).
[22] K. Belczynski, R. E. Taam, V. Kalogera, F. Rasio, and T. Bulik, Astrophys. J. **662**, 504 (2007).
[23] A. Akmal, V. R. Pandharipande, and D. G. Ravenhall, Phys. Rev. C **58**, 1804 (1998).
[24] A. W. Steiner, J. M. Lattimer, and E. F. Brown, Astrophys. J. **722**, 33 (2010).
[25] N. K. Glendenning, Astrophys. J. **293**, 470 (1985).
[26] V. R. Pandharipande and R. A. Smith, Nucl. Phys. **A237**, 507 (1975).
[27] M. Punturo *et al.*, Classical Quantum Gravity **27**, 084007 (2010).
[28] L. Lindblom, B. J. Owen, and D. A. Brown, Phys. Rev. D **78**, 124020 (2008).
[29] K. D. Kokkotas and G. Schaefer, Mon. Not. R. Astron. Soc. **275**, 301 (1995).